Density functional study of the adsorption of K on the Ag(111) surface

K. Doll
Institut für Mathematische Physik, TU Braunschweig, Mendelssohnstraße 3, D-38106 Braunschweig

Full-potential gradient corrected density functional calculations of the adsorption of potassium on the Ag(111) surface have been performed. The considered structures are Ag(111)($\sqrt{3}\times\sqrt{3}$)R30°-K and Ag(111)(2×2)-K. For the lower coverage, fcc, hcp and bridge site; and for the higher coverage all considered sites are practically degenerate. Substrate rumpling is most important for the top adsorption site. The bond length is found to be nearly identical for the two coverages, in agreement with recent experiments. Results from Mulliken populations, bond lengths, core level shifts and work functions consistently indicate a small charge transfer from the potassium atom to the substrate, which is slightly larger for the lower coverage.

I. INTRODUCTION

The study of adsorbates on metal surfaces has become a center of interest in surface science because of the enormous importance of catalysis for industrial applications. These experimental studies can be complemented with simulations which are nowadays a powerful tool for the theoretical description of surface structures and chemical reactions at surfaces, because of the growth in computational power and due to the success of density functional calculations.

One prototype reaction is the adsorption of alkali metals on metallic surfaces. Although this is a relatively simple reaction, there have been several surprises in the study of these systems. Initially, it was assumed that the adatoms would occupy hollow sites, until a first system was discovered where top site adsorption was preferred[1]. Meanwhile, further systems of alkali metals with top site adsorption have been found — typically heavier alkali atoms (from K on) on close packed surfaces (for reviews, see, e.g., references 2, 3, 4, 5, 6, 7). One important finding was that top site adsorption was accompanied by substrate rumpling and thus it was assumed that substrates with a low bulk modulus would be prominent for top site adsorption. It was therefore a little surprise when in a LEED (low energy electron diffraction) study of K on Ag(111) it was discovered that hollow sites were occupied[8,9].

The type of hollow site occupied in the system K/Ag(111) depends on the coverage: in the low coverage structures ((2 × 2) and (3×3)), the adatoms occupy face centered cubic (fcc) hollow sites, in the ($\sqrt{3}$ × $\sqrt{3}$)R30° structure the hexagonal close packed (hcp) hollow sites[8,9]. In addition, the phase diagram of K, Rb and Cs adsorbed on Ag(111) was investigated experimentally[10].

There have been several simulations of alkali metals on close-packed metallic surfaces: for example, systems such as Na and K on the Al(111) surface[11], Na on the Cu(111) surface[12], K on the Pt(111) surface[13] and K on Cu(111)[14] have been studied. The system K/Ag(111) is therefore a very interesting system due to the experimental findings and as an extension of the employed technology (section II) to substrates of the second row of the transition metals.

It is therefore the aim of this article to summarize results from simulations on the system K/Ag(111). Full-potential density-functional calculations with a local Gaussian basis set and with a gradient corrected functional were performed, for two coverages (1/3 or 1/4 of a monolayer, for a ($\sqrt{3}\times\sqrt{3}$)R30° or (2 × 2) pattern). The addressed questions are the preferred adsorption sites, the magnitude of the energy splitting of different highly symmetric adsorption sites, the geometry and the importance of surface rumpling, the charge of the adsorbate, the work function and the positions of the K core levels.

II. COMPUTATIONAL PARAMETERS

A local basis set formalism was used where the basis functions are Gaussian type orbitals centered at the atoms as implemented in the code CRYSTAL[15]. For Ag, a relativistic small-core pseudopotential (with 28 electrons in the core) in combination with a [4*s*3*p*2*d*] basis set was employed as in a previous study of Cl on Ag(111)[16]. The [5*s*4*p*1*d*] K all-electron basis from reference 14 was chosen. The exchange-correlation potential was fitted with auxiliary basis sets as in previous work[14,16]. The gradient corrected exchange and correlation functional of Perdew, Burke and Ernzerhof (PBE)[17] was used.

The adsorption was modeled by using slabs of 4 or 5 silver layers, at the PBE-optimized bulk Ag lattice constant[16] of a_0 = 4.10 Å. Potassium was adsorbed on one side of this slab. A supercell approach with a ($\sqrt{3}\times\sqrt{3}$)R30° or (2×2) structure as in the experiment was implemented. This slab was truly two dimensional and thus *not* periodically repeated in the third dimension. The vertical relaxation of the silver atoms was simulated in three different ways: simulations were performed where only a uniform relaxation of the top silver layer was possible, and simulations where a different vertical relaxation of the silver atoms in the top layer was possible (i.e. substrate rumpling). Finally, an additional

lateral displacement of the atoms in the top silver layer, as observed experimentally for K/Ni(111)[18], was simulated.

Four adsorption sites were considered (see figures 1 and 2): the top adsorption site with K sitting vertically above a silver atom in the top layer, the bridge site with K sitting above the middle of two silver atoms in the top layer, and two different threefold hollow sites where the potassium atoms are placed vertically above a silver atom in the second (third) silver layer (hcp and fcc hollow, respectively). In addition, the possibility of a stacking fault was investigated. In this structure, the outermost Ag layer and the K layer would occupy hcp sites. Such a stacking fault was observed[19] for the system Ag(111) $(\sqrt{3}\times\sqrt{3})$R30°-Sb.

The optimized geometrical parameters are defined as in figure 3. The variables are chosen in such a way so that the notation is consistent with those from the experimental references[8,9]. The bond length is defined as the distance from a potassium adatom to the nearest silver atom. d_{K-Ag1}, $d_{Ag1-Ag2}$, $d_{Ag2-Ag3}$ and $\delta 1$ are various interlayer distances: d_{K-Ag1} is the vertical distance from the potassium layer to the plane made of the atoms in the first silver layer which have moved towards the potassium layer. $d_{Ag1-Ag2}$ is the distance between the plane made of the atoms in the first layer which have moved towards the second Ag layer, and the second Ag layer. $d_{Ag2-Ag3}$, the distance between second and third layer silver atoms, was kept fixed at the value of $4.10/\sqrt{3}$ Å corresponding to the distance of two layers in the bulk ($a_0/\sqrt{3}$). Finally, $\delta 1$ is the rumpling, i.e. the distance between the plane made of those atoms in the first silver layer which have moved towards the K atoms and the plane made of those atoms in the first silver layer which have moved towards the second silver layer. Additionally, the possibility of a lateral displacement of the atoms in the top Ag layer was taken into account (for a more detailed description of the lateral displacement, see the following section III).

A net with 16×16 sampling points in the surface Brillouin zone was used[20]. During the optimization process, the Fermi function was smeared with a temperature of 0.03 E_h ($1E_h$=27.2114 eV) and the total energy extrapolated to zero temperature[21]. To ensure the stability of the results with respect to this parameter, additional single-point calculations with a smearing temperature of 0.005 E_h were performed (see also appendix). Also, the results for properties such as Mulliken population, work function etc. were computed with a smearing of 0.005 E_h. For an extensive test of the various computational parameters for metallic systems with the CRYSTAL code, see also reference 22.

The unit cells which are used in the simulations for this article are at the limit of what is presently feasible with this method. This local basis set approach is thus for metals probably more expensive than alternative approaches relying on plane wave technologies. However, it is interesting to have the possibility of comparing various strategies which complement each other. One advantage of the method employed here is that concepts such as computing Mulliken charges are easily implemented in a code relying on Gaussian basis sets. Also, all-electron calculations do not pose a problem, and although in the present work a small-core pseudopotential was used for Ag, an all-electron description would also have been possible. The usage of a pseudopotential has the advantage that scalar-relativistic corrections can be included.

III. RESULTS AND DISCUSSION

A. Ag(111) $(\sqrt{3}\times\sqrt{3})$R30°-K

In this section, the results of the calculations on the system Ag(111) $(\sqrt{3}\times\sqrt{3})$R30°-K are presented and discussed.

In table I, the adsorption geometries and energies are displayed. It turns out that all considered adsorption sites are virtually degenerate — the best calculations indicate that the binding energies for the various sites are within 0.1 mE_h which is at the limit of the numerical noise. These findings are thus no contradiction to the experiment where the hcp hollow site was identified as the preferential site. The degeneracy is certainly within the range of the errors associated within the calculation (lack of basis functions with higher angular momentum than $l=2$, number of Ag layers considered in the slab model, uncertainties in the functional, anisotropic vibrations observed in the experiment). The total computed binding energy per K atom is 0.042 E_h, i.e. 1.1 eV.

The structure with a stacking fault is also degenerate, and thus cannot be ruled out by the simulations. In agreement with a recent calculation[23], the clean Ag(111) surface with a stacking fault was found to be slightly higher in energy (by about 0.00015 E_h per atom) than the unfaulted surface.

When considering the optimal geometry for the hcp site, we note that the computed distances are in excellent agreement with the experiment: the distance between the potassium layer and the top silver layer d_{K-Ag1} was found to be 2.79 Å versus 2.84 ± 0.03 Å in the experiment[8] and the distance between first and second silver layer $d_{Ag1-Ag2}$ was obtained to be 2.37 Å (exp.: 2.35 ± 0.02 Å). This computed distance is identical to the distance in Ag bulk ($4.10/\sqrt{3}$ Å, with the PBE functional[16]), i.e. no relaxation of the top layer was found. The distance between potassium and the nearest silver atom was found to be 3.27 Å (exp.: 3.29 ± 0.02 Å). We can thus deduce an effective potassium radius of $3.27-\frac{4.10}{\sqrt{8}}$Å=1.82 Å, in agreement with the experimental value[2] of 1.82 ± 0.03 Å.

The most complex structure included the possibility of surface rumpling and of lateral relaxation of the top Ag layer. Rumpling is allowed by symmetry for the bridge and top adsorption site, and in both cases a large value

$\delta 1$ for the rumpling is obtained (0.10 Å for the bridge site and 0.22 Å for the top site). The effect of the rumpling is to push the Ag atom under the adatom deeper into the bulk, whereas the atom(s) not under the K atom move out of the bulk towards the K layer.

The importance of rumpling in the second Ag layer under the K layer was investigated for the hcp hollow site, where this is allowed by symmetry. An optimal displacement of 0.01 Å of the Ag atom vertically under the K atom, away from the K atom, was found, with an energy gain of 0.1 mE_h. In the experiment, a displacement of 0.02 ± 0.02 Å towards the K adsorbate layer was found for the Ag atom in the second layer under the K atom. Although the computed result deviates thus slightly from experiment, it is important that the energy gain is fairly small so that second layer rumpling does not appear to have a huge influence on the results (this was suggested in reference 8 as a possible reason for the switch in adsorption site).

Lateral displacement in the top Ag layer plays only a minor role, and lowers the energy at most by 0.4 mE_h. The atoms nearest to the K adsorbate were allowed to move and the lateral movement of the atoms was in all cases away from the adsorbate, by a maximum of 0.04 Å.

We also note by comparing the results for 4 layers with and without surface rumpling, that the rumpling is most important for the top site: the energy gain by rumpling is 2.5 mE_h, and 0.5 mE_h for the bridge site. This is in line with previous calculations for K/Cu(111)[14].

B. Ag(111) (2×2)-K

In the following table II, results for the Ag(111)(2×2)-K structure are displayed. Fcc hollow, hcp hollow and bridge site are within 0.2 mE_h, i.e. practically degenerate. The structure with a stacking fault is $\sim$ 0.8 mE_h higher in energy, the top site by $\sim$ 1.8 mE_h. Similar as for the higher coverage, it can only be stated that these findings are compatible with the experiment, but a statement about the preferred site is not possible.

The geometry is in good agreement with experiment: a value for the interlayer distance d_{K-Ag1} of 2.60 Å (exp.: 2.70 ± 0.03 Å) was obtained and an interlayer distance $d_{Ag1-Ag2}$ between the first and second silver layer of 2.35 Å (exp.: 2.34 ± 0.02 Å). Surface rumpling is important and a value of $\delta 1$ =0.11 Å was computed (exp.: 0.10 ± 0.03 Å). The effect of the surface rumpling was again to push those atom(s) under the potassium adsorbate deeper into the substrate, whereas the other atom (three atoms in the case of the top site, two atoms in the case of the bridge site and one atom in the case of the threefold hollow sites) move outwards towards the potassium layer.

Lateral relaxation plays a minor role for the binding energy. In all cases except for the top site where this is not possible, the atoms nearest to K move away from the K atom; in the case of the top site, the three atoms not under the K atom move slightly towards each other, away from the K atom. However, the energy gain is at the limit of the numerical accuracy.

For comparison, calculations without surface rumpling were performed, i.e. $\delta 1$ was kept fixed at 0 Å. We note that the interlayer distances d_{K-Ag1} between K layer and top Ag layer increase when rumpling is not possible, and are 2.73 Å for fcc and hcp site. The interlayer distance between first and second Ag layer hardly changes. The adsorption energy differs by $\leq 1 mE_h$ for fcc, hcp, bridge site and for the structure with a stacking fault; but by 2.9 mE_h for the top site. Thus we find again that surface rumpling is most important for the top site, however, it is not big enough to make the top site the preferred adsorption site.

The computed adsorption energy per potassium atom for this structure is 0.041 E_h, i.e. nearly identical to the higher coverage. This energy is close to the one computed for K/Al(111); also the splitting between various sites was found to be of the order of few hundreths of an eV only[11]; the binding energy is also comparable to Cu(111)(2×2)-K[14]. The adsorption energy is however lower than the one computed for K/Pt(111) where values of 2.42 eV (at a coverage of one third of a monolayer) and 2.93 eV (at a coverage of one fourth of a monolayer) were obtained, at the level of the local density approximation[13]. The energy splitting between fcc and hcp site was computed to be 15 meV in the latter publication, with the hcp site being lower; this is compatible with the near-degeneracy which is found here for the system K/Ag(111).

Finally, we also see that the results are well converged with respect to the number of layers, for both coverages: in one case (substrate rumpling, no lateral relaxation), the optimization has been performed with 4 and 5 Ag layers, and both geometry and adsorption energies are stable.

C. Population and density of states

In table III, Mulliken charges for the potassium atom are given, projected on the different basis functions. These charges are defined as

$$N_A = \sum_{\mu \in A} \sum_{\nu} P_{\mu\nu} S_{\nu\mu}$$

with density matrix P, overlap matrix S and A the set of basis functions for which the population is computed.

It should be mentioned that a relatively large number of digits has been given; although the absolute values will not be more accurate than to one or two decimal points, for the relative values more digits are still meaningful.

In the case of Ag(111) $(\sqrt{3} \times \sqrt{3})$R30°-K, the total charge is $\sim$ 0.16 $|e|$, in the case of Ag(111) (2×2)-K $\sim$ 0.24 $|e|$. Obviously, if the charges were the same, the electrostatic repulsion at higher coverage (Ag(111)

($\sqrt{3}\times\sqrt{3}$)R30°-K) would be larger because of the shorter K-K distances. Therefore, the charge in the case of Ag(111) ($\sqrt{3}\times\sqrt{3}$)R30°-K is reduced, in agreement with the Langmuir-Gurney model. The individual populations are very similar to Cu(111) (2 × 2)-K: p_x, p_y and p_z charges are slightly above 4, the number of s-electrons is ∼ 6.5; charges in p_x and p_y orbitals are identical except for the bridge site; the p_x orbital which has more overlap with the substrate layer (in our choice of geometry) is slightly less occupied than the p_y orbital. The higher occupancy of that orbital, which has less overlap with the substrate, indicates that the bond is not covalent. In addition, the overlap population defined as
$\sum_{\mu\in A}\sum_{\nu\in B} P_{\mu\nu}S_{\nu\mu}$,
with A the set of basis functions on the first atom and B the set of basis functions of the other atom, was computed. This number is a measure for covalency, and is, similar to Cu(111)(2×2)-K, very small: for K and nearest neighbor Ag, it is $\leq 0.06\ |e|$ for both coverages, and negligible for further neighbors.

In figures 4 and 5, the density of states (DOS), projected on the potassium basis functions, is displayed for the fcc adsorption site. The Fermi energy is in a regime with a significant contribution from K 4s and 4p bands, so that the overlayer is clearly metallic. The projected DOS does not depend on the adsorption site: it looks virtually identical for fcc hollow, hcp hollow, bridge and top site, and also for the structure with stacking fault. This is as found for Cu(111)(2 × 2)-K, but different from the case of chlorine as an adsorbate, where the projected DOS clearly depended on the adsorption site[16].

The values of the K 3s and 3p levels are practically independent of the adsorption site (see table IV). This is again in contrast to chlorine: for chlorine, the core eigenvalue depended on the adsorption site, and it was correlated with the charge of the chlorine atom[16]. For K, the variation of the Mulliken charges with adsorption site for fixed coverage is much smaller (table III) as for chlorine. This is thus consistent with the finding that the core eigenvalues do not vary for the different sites. Also, the position of the Fermi energy and thus the value of the work function is independent of the site, and changes slightly with the coverage.

D. Comparison of the results for the two coverages

When comparing the results for the two coverages, we firstly note that the bond lengths for the individual sites are very similar for both coverages. The bond length increases with the number of nearest neighbors to which the potassium adatom bonds, in agreement with Pauling's argument[24] that a smaller number of bonds leads to a stronger individual bond and a shorter bond length: the bond length is shortest for the top site with 2.95 Å for the ($\sqrt{3}\times\sqrt{3}$) structure (or 2.89 Å for the (2 × 2) structure), longer for the bridge site and longest for the threefold hollow sites. Similarly, the effective K radius, obtained from the difference of bond length and effective silver radius ($\frac{4.10}{\sqrt{8}}$Å), increases in this order. If we keep the Ag radius fixed, it increases from 1.50 Å (or 1.44 Å for the (2×2) structure) for the top site to 1.82 Å (or 1.76 Å) for the threefold hollow sites. These values are compatible with effective K radii deduced from experiment (see table 10 in reference 2).

In table V, the most important results of the calculations for the two coverages and the fcc hollow are compared.

The binding energy per K atom, with respect to free K atoms and a clean Ag(111) slab, is 0.042 and 0.041 E_h, i.e. nearly identical for both coverages. In the case of Ag (111) ($\sqrt{3}\times\sqrt{3}$)R30°-K, all considered sites, and in the case of Ag(111) (2 × 2)-K, the fcc, hcp and bridge site are virtually degenerate. This degeneracy was already observed in the early study of K/Al(111)[11] and explained with the fact that the large radius of potassium leads to a large distance of the adsorbate to the substrate and therefore the K adsorbate will experience only a small substrate electron density corrugation; similarly the potassium overlayer is metallic and its electronic charge more diffuse than the charge of, e.g. chlorides[25,16] or oxides[23] as adsorbates which also helps to reduce the energy difference between the threefold hollow sites and bridge or top site, compared to halogenides or oxides.

The K charge hardly depends on the adsorption site, but it depends on the coverage. The slightly higher charge (i.e. less electrons) for the lower coverage is consistent with the slightly shorter bond length and smaller effective K radius for this adsorbate system.

The values of the K 3s and 3p core eigenvalues also indicate that there is a little difference between the two coverages: For the lower coverage, the core eigenvalues are at 1.194 E_h and 0.590 E_h below the Fermi level, for the higher coverage at 1.184 E_h and 0.600 E_h. These values are virtually independent of the adsorption site. Again, this is consistent with the finding that the K charge is larger for the lower coverage and therefore the core eigenvalues are lower (i.e. there is slightly less electronic charge to screen the nuclear charge and the core levels are thus further stabilized).

The work function decreases from 0.131 E_h for the clean Ag(111) surface to 0.062 E_h for the (2 × 2) structure and increases again slightly to 0.069 E_h for the ($\sqrt{3}\times\sqrt{3}$)$R30$ structure. This finding is in line with the argument that initially, the work function will decrease linearly with increasing coverage, up to a minimum, and finally increase again because of the depolarization of the adsorbate (see, e.g. ref. 5).

Comparing the results for K/Ag(111) with K/Cu(111) and the (2 × 2) pattern, we note that the site has switched from top to the threefold hollow or bridge site. The reason appears to be that, without rumpling, the energy splitting between hollow or bridge sites and top site is less than 1 mE_h for K/Cu(111)[14], but 4 mE_h for

K/Ag(111). Substrate rumpling changes this splitting in favor of the top site; however, the change is not large enough to stabilize the top site as the ground state for K/Ag(111). The parameter most important for the magnitude of the energy splitting of the sites, without rumpling, appears to be the nearest neighbor spacing of the substrate: for a fixed radius of the K adsorbate, the adsorbed atom will have more overlap with more substrate atoms, if the substrate atoms are closer. In the case of the top site, the K atom has a nearest neighbor vertically below and six next nearest neighbors in the first layer. These six atoms are closer in the case of K/Cu(111) than K/Ag(111) because of the smaller atomic radius of copper and thus smaller lattice constant of Cu. Thus, the energy splitting is smaller for K/Cu(111) compared to K/Ag(111), and substrate rumpling can change it in favor of the top site for K/Cu(111). This argument would also hold for the system K/Ru(0001)[26] which behaves similar to K/Ag(111). The calculations thus support the argument given, for example, in reference 2 and which was based on a large set of experimental data (when varying the adsorbate, the ratio of the radius of the adsorbate to the nearest neighbor spacing of the substrate was recommended as a parameter to predict the adsorption site). In the simulations performed here, this argument can be verified by comparing the results from a surface without substrate rumpling and a surface with rumpling.

For substrates with similar lattice constants, an additional parameter will be the energy required for the deformation of the surface; this energy is found to be 1.5 mE_h for K/Cu(111) and 2.8 mE_h for K/Ag(111), for the top site ((2 × 2) structure, the energy difference between the unrelaxed clean surface and the optimal geometry of the adsorbate system, without K adsorbate, was computed). Note that the magnitude of the rumpling is larger for K/Ag(111), which may explain the higher energy necessary for the deformation of the clean Ag surface (although Ag has a lower bulk modulus than Cu).

We also note that the top site is slightly better in energy for the higher coverage than for the lower coverage, relative to the other sites (in line with the case of K/Al(111)[11]). This could be due to the larger radius of the K adsorbate for the higher coverage. As explained earlier, the positive K charge is smaller for the higher coverage and thus the radius is larger. Therefore, the overlap with the 6 nearest neighbors will be larger and the top site will be slightly more stabilized. However, this argument must be contrasted with the case of Cs/Ru(0001)[27] where the site switches from top ((2 × 2) structure) to hcp ($(\sqrt{3} \times \sqrt{3})$R30° structure). In the latter case, a better screening was suggested as the possible explanation. These two controversial findings for similar systems demonstrate how difficult it is to give even only qualitative rules for the preferred adsorption site.

We can thus give a reasonable argument for the question, why the top site is not preferred for K/Ag(111), in contrast to K/Cu(111). The question of the site switch from fcc to hcp, however, can not yet be answered. The difficulty results from the small energy splitting, and thus large number of effects on this energy scale that are possible, and may influence the site preference (e.g. slightly different charge, screening, second layer rumpling, stacking fault). Numerically, the energy splitting is at the limit of the numerical noise.

IV. SUMMARY

In summary, the impact of the article is twofold: firstly, the technology of using Gaussian type basis functions was shown to be capable of describing the adsorption on metallic surfaces. Secondly, some of the experimental findings could be confirmed (essentially the geometry), and new data could be provided (energy splitting between the various adsorption sites, Mulliken charges, core eigenvalues, work functions, and the dependence of these parameters on the coverage).

In more detail, it has been shown that density functional calculations can reproduce a part of the experimental findings for the systems Ag (111) ($\sqrt{3}\times\sqrt{3}$)R30°-K and Ag(111) (2×2)-K. The computed geometry is in excellent agreement with the experimental results, and therefore much better than for the case of K/Cu(111) where there was a deviation of ~ 0.2 Å between the experiment and the simulation[28,14]. This agreement for K/Ag(111) thus helps to support the validity of the approach employed in the simulations.

The adsorption site was found to be nearly degenerate for various sites considered for both coverages, and a value of 0.04 E_h was obtained for the binding energy. The main difference to the system K/Cu(111), where the top site is occupied, appears to be due the different lattice constant of Cu vs. Ag. In both cases, a threefold hollow site would be favored without substrate rumpling, but only in the case of K/Cu(111), the energy gain associated with the rumpling is large enough to lead to a change of the adsorption site and makes the top site favorable.

The computed energies demonstrate that various sites are virtually degenerate, within the accuracy of the calculations. This appears to be due to the metallic nature of the overlayer and the large radius of the potassium adsorbate, which makes the surface electron-density corrugation have only little impact on the energy splitting between the various sites. Possible suggestions for the change in adsorption site from fcc to hcp were tested (second layer rumpling, stacking fault). However, second layer rumpling did not have a huge impact, and the energy of the structure with a stacking fault was still degenerate with the other structures, within the accuracy of the calculations. It is therefore possible to give arguments why the top site is not occupied, but the question of the site change from fcc to hcp remains puzzling. The near-degeneracy of the energies indicates that minute effects are responsible for the site change.

The computed potassium charge is between +0.16 $|e|$ for the higher and +0.24 $|e|$ for the lower coverage. These charges are consistent with results for the effective K radius and K-Ag bond length which increase for the higher coverage, with the work function, and with the K $3s$ and $3p$ core eigenvalues which move slightly closer to the Fermi energy for the higher coverage. This consistency indicates that Mulliken charges are a simple and useful concept for describing adsorption on metallic surfaces. As in the case of K/Cu(111), the small overlap population indicates that virtually no evidence can be found for a covalent contribution to the binding.

*

APPENDIX A: NUMERICAL INTEGRATION

The accuracy of the numerical integration depends especially on the number of sampling points and the smearing temperature employed. Obviously, a higher number of sampling points will lead to a higher accuracy. The optimal smearing temperature will depend on the band structure and on the number of $\vec{k}$-points. In general, a lower smearing temperature will be better because the Fermi function (which is a step function at zero temperature and thus makes accurate integration numerically difficult) is better approximated. However, when quantities such as susceptibilities are computed, the smearing temperature should not be too low, because the function to be integrated has singularities (see, e.g., the discussion in reference 21).

To investigate the dependence of the results on the smearing temperature, first a simple test was performed where the lattice constant of bulk Ag was optimized at $T = 0.005 E_h$. The optimal lattice constant was 4.12 Å, the cohesive energy 0.090 E_h and the bulk modulus 108 GPa. At a higher temperature of $T = 0.03 E_h$, the optimized values were[16] 4.10 Å, 0.088 E_h and 113 GPa. The higher smearing temperature of 0.03 E_h thus does not seem to have a huge impact on the result. This is also seen in the comparison in tables I and II, where the energy splitting between the various sites hardly changes when the smearing temperature is reduced from 0.03 E_h to 0.005 E_h. There is a change in the total binding energy, which is however still negligible compared to its magnitude.

Finally, in figure 6, the binding energy $E_{K/Ag(111)} - E_K - E_{Ag(111)}$ is computed for the hcp site, with a 3 layer slab simulating the Ag(111) surface. It becomes obvious that the binding energy depends similarly on the number of $\vec{k}$-points as on the smearing temperature. As a whole, it can be concluded that the employed smearing temperature should not lead to serious errors for the results presented in this article.

[1] S. Å. Lindgren, L. Walldén, J. Rundgren, P. Westrin and J. Neve, Phys. Rev. B **28**, 6707 (1983).
[2] R. D. Diehl and R. McGrath, Surf. Sci. Rep. **23**, 43 (1996).
[3] R. D. Diehl and R. McGrath, J. Phys.: Condensed Matter **9**, 951 (1997).
[4] H. Over, Progr. in Surf. Sci. **58**, 249 (1998).
[5] A. Zangwill, Physics at Surfaces, University Press, Cambridge (1988).
[6] C. Stampfl and M. Scheffler, Surf. Rev. Lett. **2**, 317 (1995).
[7] M. Scheffler and C. Stampfl, in: Handbook of Surface Science, Vol. 2: Electronic Structure, Editors: K. Horn and M. Scheffler, Amsterdam (1999).
[8] G. S. Leatherman, R. D. Diehl, P. Kaukasoina and M. Lindroos, Phys. Rev. B **53**, 10254 (1996).
[9] P. Kaukasoina, M. Lindroos, G. S. Leatherman and R. D. Diehl, Surf. Rev. Lett. **4**, 1215 (1997).
[10] G. S. Leatherman and R. D. Diehl, Phys. Rev. B **53**, 4939 (1996).
[11] J. Neugebauer and M. Scheffler, Phys. Rev. B **46**, 16067 (1992).
[12] J. M. Carlsson and B. Hellsing, Phys. Rev. B **61**, 13973 (2000).
[13] S. Moré, W. Berndt, A. M. Bradshaw, and R. Stumpf, Phys. Rev. B **57**, 9246 (1998).
[14] K. Doll, Euro. Phys. J. B **22**, 389 (2001).
[15] V. R. Saunders, R. Dovesi, C. Roetti, M. Causà, N. M. Harrison, R. Orlando, C. M. Zicovich-Wilson, CRYSTAL 98 User's Manual, Theoretical Chemistry Group, University of Torino (1998).
[16] K. Doll and N. M. Harrison, Phys. Rev. B **63**, 165410 (2001).
[17] J. P. Perdew, K. Burke and M . Ernzerhof, Phys. Rev. Lett. **77**, 3865 (1996).
[18] D. Fisher, S. Chandavarkar, I. R. Collins, R. D. Diehl, P. Kaukasoina and M. Lindroos, Phys. Rev. Lett. **68**, 2786 (1992).
[19] E. A. Soares, C. Bittencourt, V. B. Nascimento, V. E. de Carvalho, C. M. C. de Castilho, C. F. McConville, A. V. de Carvalho and D. P. Woodruff, Phys. Rev. B **61**, 13983 (2000).
[20] J. D. Pack and H.J. Monkhorst, Phys. Rev. B **16**, 1748 (1977).
[21] M. J. Gillan, J. Phys. C **1**, 689 (1989).
[22] K. Doll, N. M. Harrison, and V. R. Saunders, J. Phys.: Condensed Matter **11**, 5007 (1999).
[23] W.-X. Li, C. Stampfl and M. Scheffler, Phys. Rev. B **65**, 075407 (2002).
[24] L. Pauling, The nature of the chemical bond and the structure of molecules and crystals, Cornell University Press (1960).
[25] K. Doll and N. M. Harrison, Chem. Phys. Lett. **317**, 282 (2000).
[26] M. Gierer, H. Bludau, T. Hertel, H. Over, W. Moritz and G. Ertl, Surf. Sci. **279**, L170 (1992).
[27] H. Over, H. Bludau, M. Skottke-Klein, G. Ertl, W. Moritz and C. T. Campbell, Phys. Rev. B **45**, 8638 (1992).
[28] D. L. Adler, I. R. Collins, X. Liang, S. J. Murray, G. S. Leatherman, K.-D. Tsuei, E. E. Chaban, S. Chandravarkar, R. McGrath, R. D. Diehl and P. H. Citrin, Phys. Rev. B **48**, 17445 (1993).

TABLE I. Adsorption of K on the Ag(111) surface, $(\sqrt{3} \times \sqrt{3})$ R30° pattern. The adsorption energy E_{ads} is the difference $E_{\mathrm{K/Ag(111)}} - E_{\mathrm{Ag(111)}} - E_{\mathrm{K}}$. For the most complex geometry, this energy was computed with two different parameters of the smearing temperature, 0.03 E_h and 0.005 E_h, for comparison.

site	*Bond length* [Å]	d_{K-Ag1} [Å]	$d_{Ag1-Ag2}$ [Å]	$\delta 1$ [Å]	lateral [Å]	$E_{ads}(0.03)$ $\left[\frac{E_h}{K\ atom}\right]$	$E_{ads}(0.005)$ $\left[\frac{E_h}{K\ atom}\right]$
			4 layers, without substrate rumpling, without lateral relaxation				
fcc hollow	3.26	2.80	2.37	0	0	-0.0442	
hcp hollow	3.26	2.80	2.37	0	0	-0.0440	
bridge	3.16	2.81	2.37	0	0	-0.0437	
top	2.94	2.94	2.37	0	0	-0.0413	
stacking fault	3.27	2.81	2.38	0	0	-0.0435	
			4 layers, with substrate rumpling, without lateral relaxation				
fcc hollow	3.26	2.80	2.37	0	0	-0.0442	
hcp hollow	3.26	2.80	2.37	0	0	-0.0440	
bridge	3.18	2.73	2.34	0.10	0	-0.0442	
top	2.96	2.73	2.24	0.23	0	-0.0438	
stacking fault	3.27	2.81	2.38	0	0	-0.0435	
			5 Ag layers, with substrate rumpling, without lateral relaxation				
fcc hollow	3.27	2.81	2.37	0	0	-0.0443	
hcp hollow	3.27	2.81	2.37	0	0	-0.0441	
bridge	3.18	2.74	2.34	0.10	0	-0.0443	
top	2.95	2.73	2.25	0.22	0	-0.0441	
stacking fault	3.27	2.81	2.38	0	0	-0.0437	
			5 Ag layers, with substrate rumpling, with lateral relaxation				
fcc hollow	3.27	2.79	2.37	0	0.04	-0.0444	-0.0422
hcp hollow	3.27	2.79	2.37	0	0.04	-0.0442	-0.0421
bridge	3.19	2.74	2.33	0.10	0.01	-0.0444	-0.0422
top	2.95	2.73	2.25	0.22	0	-0.0441	-0.0422
stacking fault	3.27	2.79	2.38	0	0.03	-0.0441	-0.0422
exp (hcp)[8,9]	3.29 ± 0.02	2.84 ± 0.03	2.35 ± 0.02	0			

TABLE II. Adsorption of K on the Ag(111) surface, (2×2) pattern. The adsorption energy E_{ads} is the difference $E_{\mathrm{K/Ag(111)}} - E_{\mathrm{Ag(111)}} - E_{\mathrm{K}}$. For the most complex geometry, this energy was computed with two different parameters of the smearing temperature, 0.03 E_h and 0.005 E_h, for comparison.

site	*Bond length* [Å]	d_{K-Ag1} [Å]	$d_{Ag1-Ag2}$ [Å]	$\delta 1$ [Å]	lateral [Å]	$E_{ads}(0.03)$ $\left[\frac{E_h}{K\ atom}\right]$	$E_{ads}(0.005)$ $\left[\frac{E_h}{K\ atom}\right]$
4 Ag layers, without substrate rumpling, without lateral relaxation							
fcc hollow	3.20	2.73	2.37	0	0	-0.0418	
hcp hollow	3.20	2.73	2.37	0	0	-0.0416	
bridge	3.11	2.75	2.37	0	0	-0.0412	
top	2.87	2.87	2.36	0	0	-0.0378	
stacking fault	3.21	2.74	2.39	0	0	-0.0409	
4 Ag layers, with substrate rumpling, without lateral relaxation							
fcc hollow	3.21	2.61	2.34	0.13	0	-0.0424	
hcp hollow	3.21	2.61	2.34	0.13	0	-0.0422	
bridge	3.12	2.64	2.31	0.12	0	-0.0422	
top	2.90	2.67	2.22	0.23	0	-0.0407	
stacking fault	3.21	2.61	2.35	0.13	0	-0.0415	
5 Ag layers, with substrate rumpling, without lateral relaxation							
fcc hollow	3.20	2.61	2.34	0.12	0	-0.0423	
hcp hollow	3.21	2.61	2.34	0.13	0	-0.0423	
bridge	3.12	2.66	2.32	0.11	0	-0.0422	
top	2.89	2.66	2.22	0.23	0	-0.0408	
stacking fault	3.21	2.62	2.35	0.12	0	-0.0415	
5 Ag layers, with substrate rumpling, with lateral relaxation							
fcc hollow	3.20	2.60	2.35	0.11	0.04	-0.0424	-0.0411
hcp hollow	3.21	2.60	2.35	0.12	0.03	-0.0425	-0.0413
bridge	3.13	2.65	2.32	0.11	0.04	-0.0425	-0.0411
top	2.89	2.66	2.22	0.23	0.005	-0.0408	-0.0395
stacking fault	3.20	2.59	2.35	0.13	0.02	-0.0417	-0.0405
exp (fcc)[8,9]	3.27 ± 0.03	2.70 ± 0.03	2.34 ± 0.02	0.10 ± 0.03			

TABLE III. Orbital-projected potassium charge for different adsorption sites (5 Ag layers, with substrate rumpling and lateral relaxation).

site	charge, in $\lvert e\rvert$				
	s	p_x	p_y	p_z	total
			$(\sqrt{3} \times \sqrt{3})$R30°		
fcc hollow	6.513	4.135	4.135	4.052	18.843
hcp hollow	6.515	4.134	4.134	4.052	18.843
bridge	6.513	4.127	4.144	4.052	18.845
top	6.502	4.146	4.148	4.051	18.856
stacking fault	6.515	4.134	4.134	4.051	18.843
			(2×2)		
fcc hollow	6.494	4.115	4.114	4.025	18.757
hcp hollow	6.496	4.114	4.114	4.025	18.757
bridge	6.496	4.106	4.122	4.027	18.760
top	6.487	4.123	4.123	4.028	18.772
stacking fault	6.496	4.114	4.114	4.025	18.757

TABLE IV. Position of the K $3s$ and $3p$ core eigenvalues, and position of the Fermi energy, in E_h (5 Ag layers, with substrate rumpling and lateral relaxation).

site	$(\sqrt{3} \times \sqrt{3})$R30°	(2×2)
fcc hollow	-1.253 ; -0.659 ; -0.069	-1.256 ; -0.662 ; -0.062
hcp hollow	-1.253 ; -0.658 ; -0.069	-1.256 ; -0.662 ; -0.062
bridge	-1.253 ; -0.659 ; -0.069	-1.257 ; -0.662 ; -0.062
top	-1.253 ; -0.659 ; -0.069	-1.258 ; -0.664 ; -0.062
stacking fault	-1.253 ; -0.659 ; -0.069	-1.256 ; -0.661 ; -0.062

TABLE V. Comparison of the results for the two coverages (fcc hollow site).

structure	$(\sqrt{3} \times \sqrt{3})$R30°-K	(2×2)-K
bond length [Å]	3.27	3.20
effective K radius [Å]	1.82	1.76
binding energy $\left[\frac{E_h}{K\ atom}\right]$	0.042	0.041
Mulliken charge on K $[\|e\|]$	0.16	0.24
K $3s$, $3p$ core eigenvalues, relative to Fermi energy $[E_h]$	-1.184 ; -0.590	-1.194 ; -0.600
work function $[E_h]$ (clean Ag(111): 0.131)	0.069	0.062

FIG. 1. The structures considered for K, adsorbed on the Ag(111) surface, at a coverage of one third of a monolayer, $(\sqrt{3}\times\sqrt{3})$R30° unit cell. The silver atoms in the top layer are displayed by open circles. The considered potassium adsorption sites are the top site above the silver atoms with number 1 (filled circles), the threefold hollow sites above atoms 1,2,3 (fcc or hcp hollow, possibly with stacking fault, circles with horizontal lines) or the bridge site above atoms 2 and 3 (circles with horizontal and vertical lines). Note that the threefold hollow sites can not be distinguished in this figure.

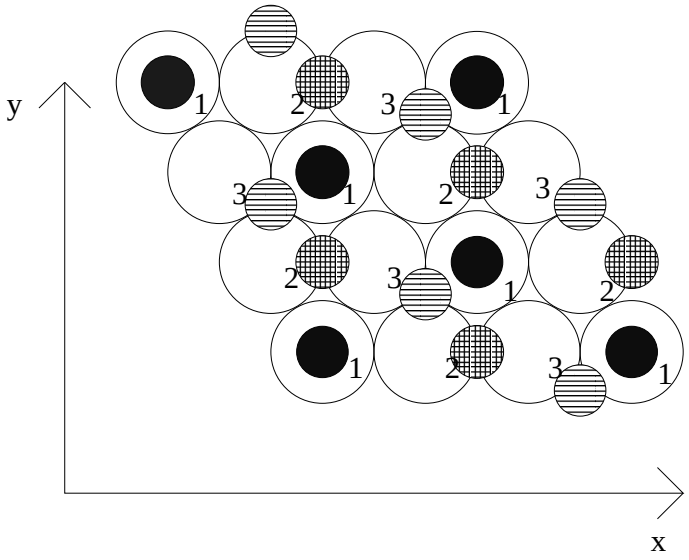

FIG. 2. The structures considered for K, adsorbed on the Ag(111) surface, at a coverage of one fourth of a monolayer, (2×2) unit cell. The silver atoms in the top layer are displayed by open circles. The considered potassium adsorption sites are the top site above the silver atoms with number 1 (filled circles), the threefold hollow sites above atoms 2,3,4 (fcc or hcp hollow, possibly with stacking fault, circles with horizontal lines) or the bridge site above atoms 3 and 4 (circles with horizontal and vertical lines). Note that the threefold hollow sites can not be distinguished in this figure.

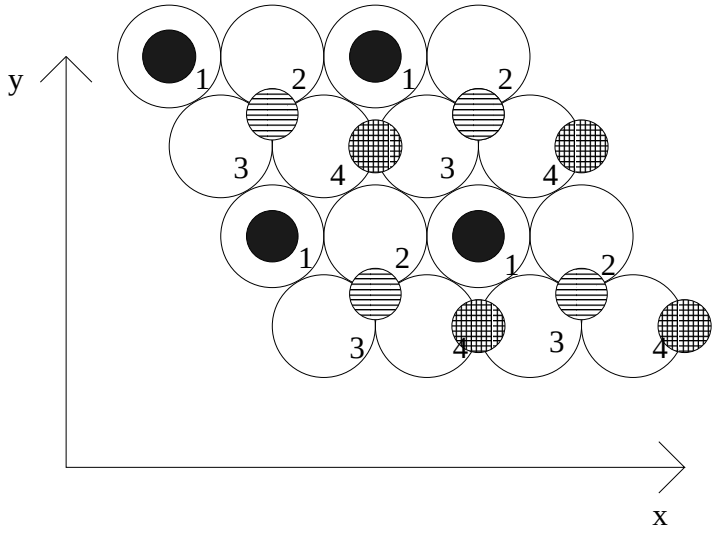

FIG. 3. Definition of the geometrical parameters. All distances are interlayer distances (definition see text). Note that in all the figures, the atoms are drawn purely schematically and the size of the atoms does not scale with the atomic radii.

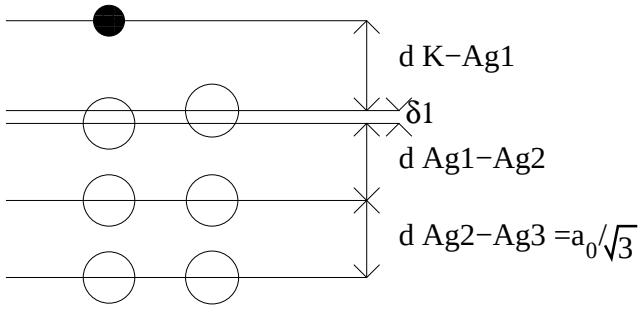

FIG. 4. DOS, projected on K, fcc adsorption site, $(\sqrt{3} \times \sqrt{3})$R30° structure. The DOS, projected on all K basis functions, is shown, together with the DOS projected on s, p_x, p_y and p_z orbitals only. The Fermi energy is indicated with a vertical line.

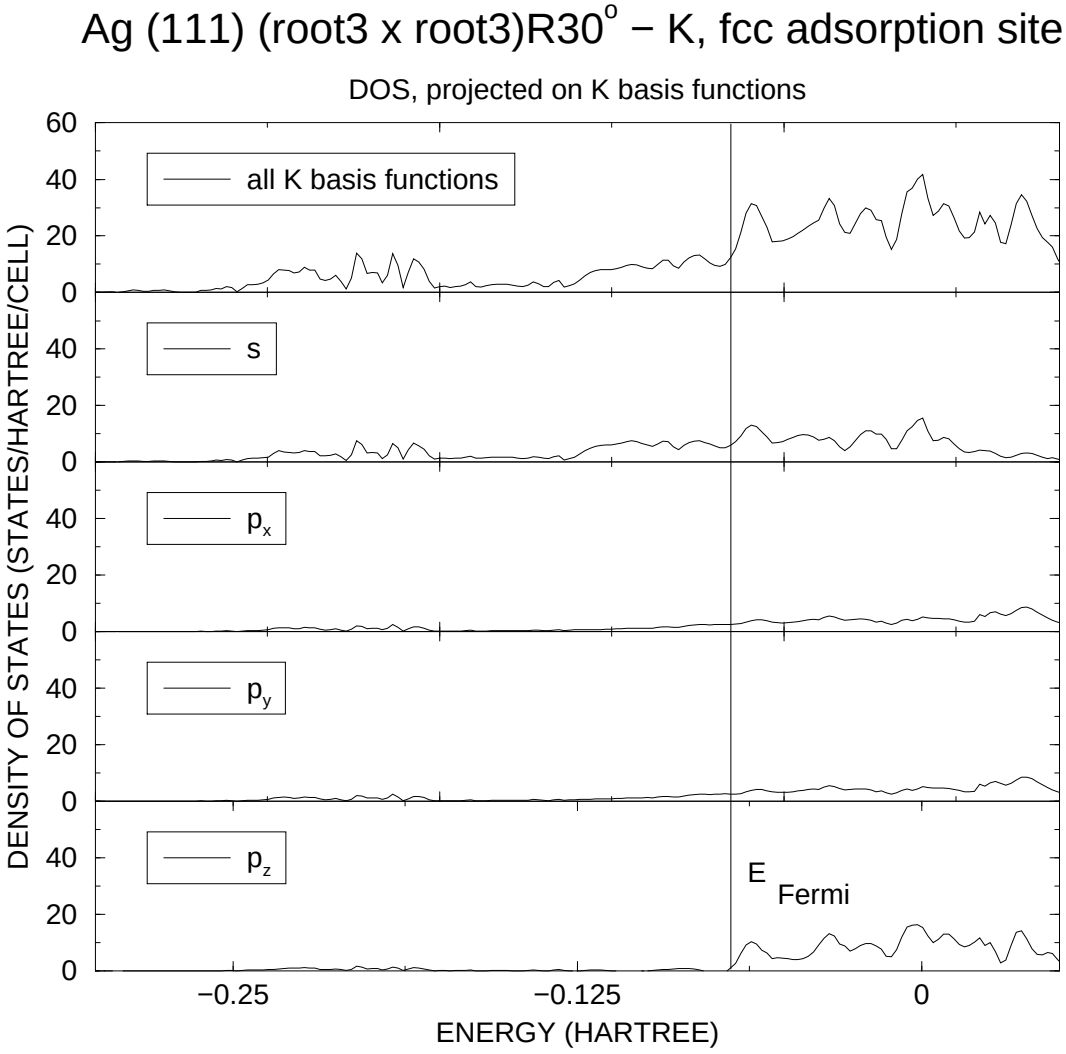

T=0.005

FIG. 5. DOS, projected on K, fcc adsorption site, (2x2) structure. The DOS, projected on all K basis functions, is shown, together with the DOS projected on s, p_x, p_y and p_z orbitals only. The Fermi energy is indicated with a vertical line.

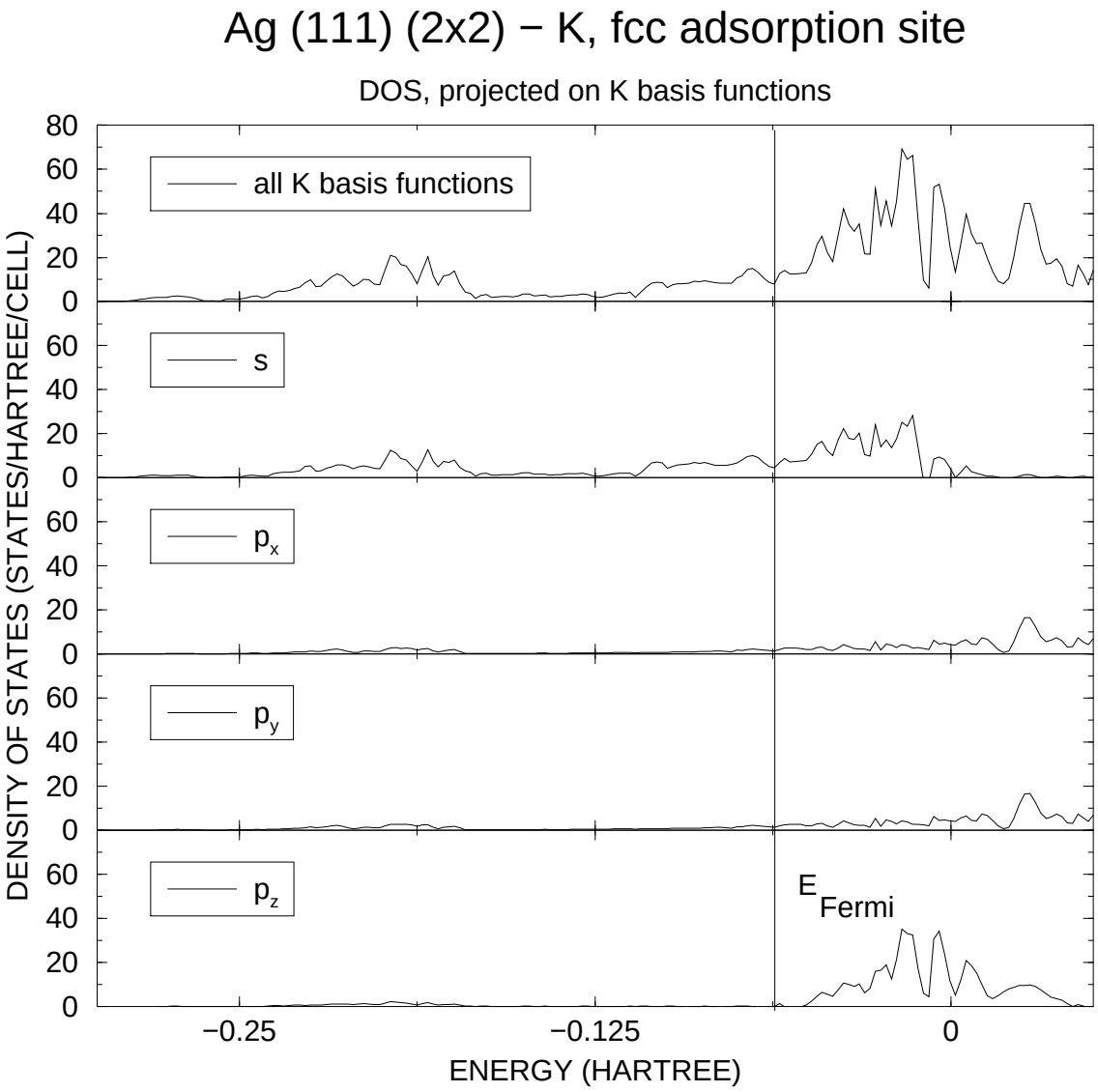

FIG. 6. Binding energy $E_{\mathrm{K/Ag(111)}} - E_{\mathrm{Ag(111)}} - E_{\mathrm{K}}$, for K adsorbed on the hcp site of the (111) surface of a 3 layer Ag slab. Various smearing temperatures from 0.001 E_h to 0.05 E_h, and $\vec{k}$-point samplings from 2×2 up to 16×16 have been compared.